Spectroelectrochemical Characterisation of poly[Ni(saltMe)]-Modified Electrodes**

Miguel Vilas-Boas,[a] Cristina Freire,*[a] Baltazar de Castro,[a] Paul A. Christensen,[b] and A. Robert Hillman[c]

Abstract: Electrogenerated polymers based on the nickel(II) complex 2,3-dimethyl-*N*,*N*′-bis(salicylidene)butane-2,3-diaminatonickel(II), poly[Ni(saltMe)], were characterised by in situ FTIR and UV/Vis spectroscopy and ex-situ EPR spectroscopy in order to gain insights into film structure, electronic states and charge conduction. The role of the nickel ions during film oxidation was probed by using EPR to study naturally abundant Ni and ^{61}Ni-enriched polymers. The data from all the spectroscopic techniques are consistent, and clearly indicate that polymerisation and redox switching are associated with oxidative ligand based processes; coulometry suggests that one positive charge was delocalised through each monomer unit. EPR provided evidence for the non-direct involvement of the metal in polymer oxidation: the polymer is best described as a polyphenylene-type compound (conducting polymer), rather than an aggregation of nickel complexes (redox polymer), and the main charge carriers are identified as polarons. An explanation for the high electrochemical stability and conductivity of poly[Ni(saltMe)] with respect to that of poly[Ni(salen)] is proposed, based on stereochemical repulsion between monomeric units; this can impose a less compact supramolecular structure on polymers with bulkier substituents.

Keywords: electroactive polymers · electrochemistry · EPR spectroscopy · nickel · Schiff bases

Introduction

The redox chemistry of [Ni(salen)]-based polymers (salen = *N*,*N*′-bis(salicylidene)ethylenediamine dianion) is a matter of current interest due to the potential application of these modified electrodes in heterogenous electrocatalysis. Previous studies of the oxidative chemistry of poly[Ni(salen)][1–8] have failed to provide an unambiguous assignment of the redox surface couple. Recently, we carried out a spectroelectrochemical characterisation of poly[Ni(salen)],[9] and have shown that the polymer, although based on a bona fide coordination compound, behaves rather like a polyphenylene. No electrochemical activity was detected that was attributable to the nickel centre, and it was postulated that the role of these centres was to establish a bridge between the biphenylene moieties, and under the moderate conditions used (potential range 0.0 – 1.0 V versus Ag/AgCl 0.1 mol dm^{-3} NaCl), the main charge carriers were proposed to be polarons.[9] The above study has provided important insights into the nature of the redox surface couple and charge carriers, but it was limited by the low stability of poly[Ni(salen)] at high doping levels, due to its irreversible over-oxidation. The spectroelectrochemical characterisation of nickel-salen based polymers at potentials higher than 1.0 V versus Ag/AgCl 0.1 mol dm^{-3} NaCl warrants further investigation.

To extend our studies in this field, and in order to electrosynthesise polymers with good electrochemical performance over a wider potential range, two possible structural modification strategies could be pursued: introducing substituents either at 1) the aldehyde moieties or 2) the imine bridge. We decided to investigate the second option, and to replace the four hydrogen atoms of the imine bridge of

[a] Dr. C. Freire, M. Vilas-Boas, Prof. B. de Castro
CEQUP/Departamento de Química, Faculdade de Ciências
Universidade do Porto
4169-007 Porto (Portugal)
Fax: (+351) 22-6082959
E-mail: acfreire@fc.up.pt

[b] Dr. P. A. Christensen
Department of Chemistry
University of Newcastle
Newcastle upon Tyne, NE1 7RU (UK)
Fax: (+44) 191-222-5472

[c] Prof. A. R. Hillman
Department of Chemistry
University of Leicester
Leicester LE1 7RH, (UK)
Fax: (+44) 116-252-5227

Supporting information for this article is available on the WWW under http://www.wiley-vch.de/home/chemistry/ or from the authors

[**] [Ni(saltMe)] = 2,3-dimethyl-*N*,*N*′-bis(salicylidene)butane-2,3-diaminatonickel(II).

  0947-6539/01/0701-0139 $ 17.50+.50/0

[Ni(salen)] with methyl groups to increase specifically the imine bridge bulkiness. The complex 2,3-dimethyl-*N*,*N*′-bis-(salicylidene)butane-2,3-diaminatonickel(II), [Ni(saltMe)] has been prepared,[10] and its oxidative chemistry in CH_3CN studied.[11] The monomer electropolymerises on Pt electrodes in CH_3CN/0.1 mol dm^{-3} TEAP (TEAP = tetraethylammonium perchlorate) and exhibits, in the potential range 0.0 to 1.3 V, a reversible oxidative electrochemical behaviour with two redox couples at $E_{1/2}(\mathrm{I}) = 0.65$ V and $E_{1/2}(\mathrm{II}) = 0.91$ V. When compared with poly[Ni(salen)], this new polymer exhibits much higher conductivity and greater stability/durability when exposed to solutions of CH_3CN/0.1 mol dm^{-3} TEAP. These properties have allowed a detailed study of the kinetics of charge propagation and redox dynamics within a polymer based on a [Ni^{II}(salen)]-type complex.[11, 12] The use of cyclic voltammetry and chronoamperometry[11] led to an estimate of the product of the diffusion coefficient and concentration of electroactive species, $D^{1/2}C$, for the second electrochemical process. The comparison of these values for the anodic and cathodic reactions, as well as their dependence on film thickness, was interpreted as arising from the entry and exit of ClO_4^- and CH_3CN between film and solution during redox switching. The combined in situ electrochemical quartz crystal microbalance and probe beam deflection technique (EQCM-PBD) provided a detailed description of the mobile species involved in the redox switching[12] and confirmed the uptake of ClO_4^- as the major contribution to charge compensation. Moreover, in the second process, ($E_{1/2}(\mathrm{II}) = 0.91$ V), significant solvent entry was observed together with anion insertion. A quantitative evaluation of the transferred species showed that two molecules of solvent were involved per anion transferred.

Coulometric studies on poly[Ni(saltMe)][11] have indicated that, for the wide potential range used, approximately one positive charge is de-localised per monomer unit. This result contrasts markedly with that of poly[Ni(salen)], for which the doping level n' was 0.62 (potential range, 0.0 – 1.0 V), which corresponds to two positive charges delocalised over three monomer units. This result provided the first indication that the oxidation of poly[Ni(salen)], was a ligand-based process.[9] For poly[Ni(saltMe)], as its oxidation degree is one, no unambiguous assignment for the polymer active site could be made on the basis of the electrochemical and physicochemical data alone. Complementary studies on the electronic structure of the films were clearly required, and a full spectroscopic characterisation is essential to achieve a clear-cut distinction between ligand- and metal-based oxidative behaviour. Additionally, the high electrochemical stability of poly[Ni(saltMe)] in the potential range 0 – 1.3 V, allows the spectroelectrochemical characterisation of the polymer at high levels of doping (at $E > 1.0$ V).

In situ ellipsometric studies[13] on the growth and electrochemical cycling of poly[Ni(saltMe)] films showed a steady decrease in the real part of the refractive index (n) at 632.8 nm during electrochemical oxidation of the as-grown film, in the region of the first oxidative process. At higher potentials, this deacrease was observed to level out. In contrast, both the imaginary part of the refractive index (k) and the thickness of the film were seen to increase on oxidation. The latter result finds a counterpart in the strong increase in mass detected by EQCM,[13] associated with solvent and anion entry into the film. The variation of n and k can be correlated with the changes in the near IR region and UV/Vis spectra of the film, respectively.

Herein we report the complete characterisation of the redox switching of poly[Ni(saltMe)] over the potential range 0.0 to 1.3 V by in situ FTIR and UV/Vis spectroscopies and ex situ EPR studies. In order to probe the role of the nickel ions during film oxidation, we have performed EPR studies using naturally abundant Ni and ^{61}Ni-enriched polymers.

Abstract in Portuguese: *Descreve-se a caracterização espectroscópica de um polímero preparado electroquimicamente a partir do complexo 2,3-dimetil-N,N′-bis(salicilidene)butano-2,3-diiminato-níquel(II), caracterização que utilizou técnicas in situ (espectroscopia de infravermelho com transformada de Fourier e de ultravioleta-visível) e ex situ (ressonância paramagnética electrónica - RPE) para obter informação sobre a estrutura do filme e dos estados electrónicos que lhe estão associados, quer no estado reduzido e oxidado, bem como sobre o mecanismo de condução. Foi também estudada a influência do catião níquel(II) no processo de oxidação, recorrendo a RPE de polímeros preparados com níquel de abundância natural e com ^{61}Ni. Os resultados fornecidos pelas diferentes técnicas espectroscópicas formam um conjunto coerente e mostram claramente que a electropolimerização e a oxidação do filme envolvem processos electroquímicos associados ao ligando, muito embora os resultados coulométricos apontem para a existência no polímero oxidado de uma carga positiva deslocalizada por unidade monomérica. A RPE confirmou o não envolvimento directo do catião metálico durante o processo de oxidação do filme, pelo que o polímero tem um comportamento que se assemelha mais ao de um composto do tipo polifenileno, um polímero condutor em que os principais transportadores de carga são polarões, do que a um polímero redox formado por um agregado de complexos de níquel. Finalmente, é avançada uma explicação para a elevada estabilidade electroquímica de poli[Ni(saltMe)] relativamente à do polímero homólogo poli[Ni(salen)] e que se baseia na existência de maiores repulsões estereoquímicas entre as unidades monoméricas causadas pelos grupos metilo da ponte de diimina que se traduzem numa estrutura supramolecular menos compacta para poli[Ni(saltMe)].*

Results and Discussion

In situ FTIR experiments: Figure 1a shows cyclic voltammograms taken during the growth of a poly[Ni(saltMe)] film on the reflective Pt electrode employed in the in situ FTIR cell, and Figure 1b shows a cyclic voltammogram of the as-grown film in fresh acetonitrile solution in the absence of the monomer. The charge under the anodic wave in Figure 1b is about 8.2 mC, compared to about 4.7 mC under the cathodic sweep, suggesting considerable charge trapping over the timescale of the cyclic voltammetry experiment.

0947-6539/01/0701-0140 $ 17.50+.50/0 *Chem. Eur. J.* **2001**, *7*, No. 1

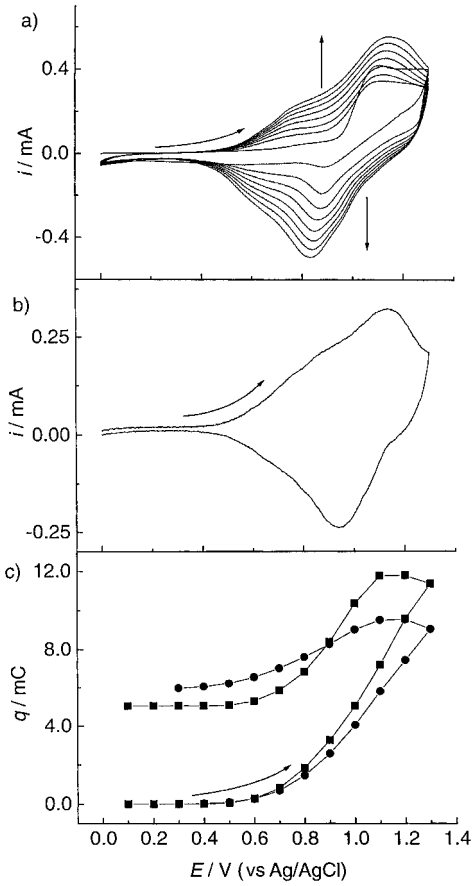

Figure 1. Cyclic voltammograms of a 0.64 cm^2 Pt disk electrode immersed in 0.1 mol dm^{-3} TEAP/CH_3CN, between 0.0 and 1.3 V at 0.1 Vs^{-1} collected during: a) the anodic polymerisation of 1 mmol dm^{-3} [Ni(saltMe)]; b) the cycling of the poly[Ni(saltMe)]-modified electrode. c) the potential dependence of the cumulative charge passed, obtained: (■) from the cyclic voltammogram in b), (●) during the FTIR experiment depicted in Figure 4.

Figure 1c shows a plot of the cumulative charge passed during the cyclic voltammetry experiment shown in Figure 1b, and for comparison the charge passed during the FTIR experiment discussed below (see Figure 4a) is also shown. There is clearly a good agreement between the two sets of data, with considerable hysteresis in the anodic and cathodic sweeps of the two experiments, and the FTIR data also supports the postulate of charge trapping. This latter observation is interesting given the considerably longer time scale over which measurements were made in the FTIR experiment, (35 s per spectrum, i.e. per data point), compared to the cyclic voltammetry, (0.10 V s^{-1} scan rate, 1 s per data point).

Figure 2 shows "absolute" in situ FTIR spectra,[9] that is, normalised to the bare platinum electrode in the CH_3CN/0.1 mol dm^{-3} TEAP, of i) the monomer, and ii) the polymer at 0.3 V; the absorbance of the monomer spectrum was increased by a factor of 6 for clarity. There are a number of significant differences between the two spectra in the ranges 1500–1300 cm^{-1} and 1170–1000 cm^{-1}. The region between 1300 and 1550 cm^{-1} of the monomer spectrum shows a broad loss feature, attributable to acetonitrile and to incomplete nulling of the solvent features. This effectively obscures any of the monomer (gain) features in this region. However, the bands at 1606, 1534 and 1328 cm^{-1} may be assigned to the

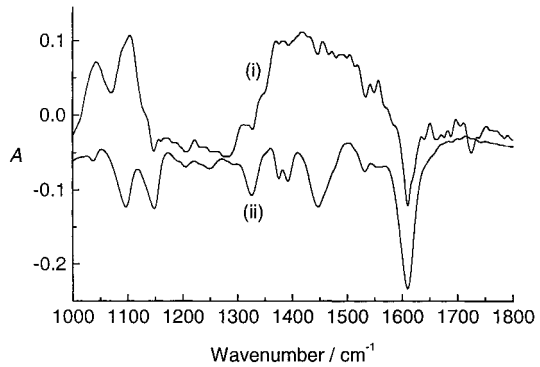

Figure 2. Absolute in situ FTIR reflectance spectra (8 cm^{-1} resolution, 100 co-added and averaged scans, 40 kHz detector speed) in 0.1 mol dm^{-3} TEAP/CH_3CN of: i) 1 mmol dm^{-3} [Ni(saltMe)]; ii) the poly[Ni(saltMe)] modified electrode depicted in Figure 1 at 0.0 V. See text for details. A = absorbance.

C=N stretching vibration, and vibrations of the chelate ring[9, 14] (see below), and clearly occur at the same frequencies in the spectra of the monomer and polymer. This suggests that the co-ordination around the nickel centre is the same in the monomer and polymer. A number of weak gain features can be discerned superimposed upon the broad acetonitrile loss feature in Figure 2 (between 1300–1500 cm^{-1}). This region covers the range over which the phenyl ring vibrations would be expected to absorb. The differences in this region between the monomer and polymer spectra suggest that polymerisation occurs through the phenyl rings, as has been observed for poly[Ni(salen)].[9] In order to try and identify the sites where polymerisation occurs in the phenyl ring, we have synthesised the homologous monomer with chloride substituents in the 3- and 5-positions of the phenyl ring, 2,3-dimethyl-*N*,*N*′-bis(3,5-dichlorosalicylidene)butane-2,3-diaminatonickel(II), [Ni(3,5-Cl_4-saltMe)], and studied its spectroelectrochemical properties. The cyclic voltammograms obtained under the same experimental conditions as for [Ni(saltMe)] (Figure 3)

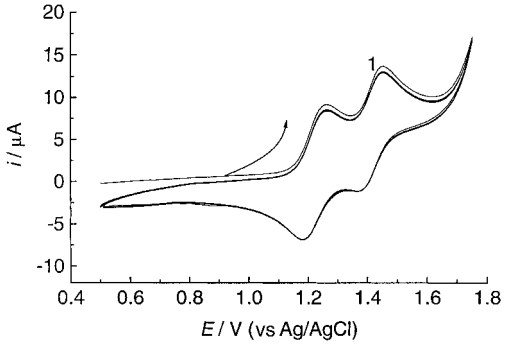

Figure 3. Cyclic voltammograms of a 0.64 cm^2 Pt electrode immersed in 1 mmol dm^{-3} [Ni(3,5-ClsaltMe)]/0.1 mol dm^{-3} TEAP/CH_3CN, between 0.0 and 1.3 V at 0.1 V s^{-1}.

show repetitive cycles and two reversible oxidation processes at $E_{1/2}(\mathrm{I}) = 1.23$ V and $E_{1/2}(\mathrm{II}) = 1.42$ V ($\nu = 0.1$ Vs^{-1}); we observe no irreversible process corresponding to polymerisation. These results indicate that polymerisation does not occur when positions 3 and 5 are blocked, and this confirms that polymerisation occurs by coupling the phenyl groups

through these positions. A more detailed study on the spectroelectrochemical characterisation of the oxidative process of this complex will be published elsewhere.[15]

Figures 4a and b show "absolute" spectra taken during the oxidation of the polymer in 0.10 V steps from 0.3 – 1.3 V. They are very similar to those observed during the oxidation of poly[Ni(salen)]: i) a broad electronic absorption grows above

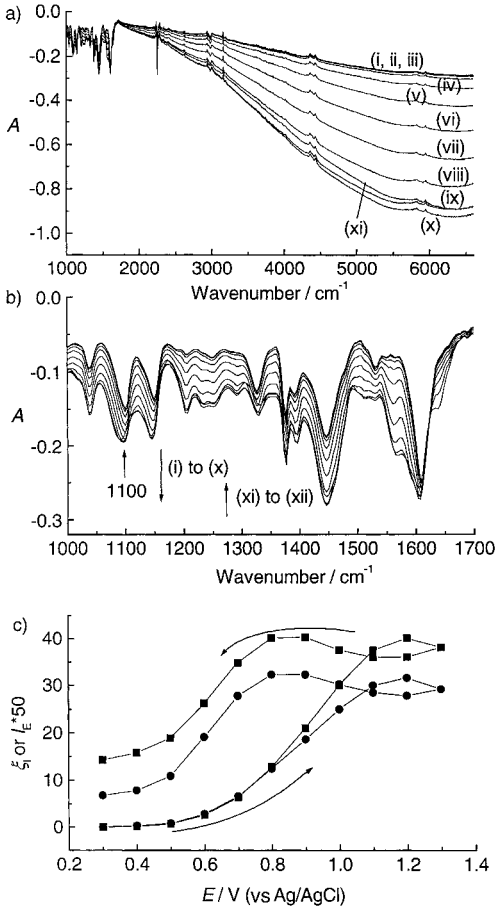

Figure 4. Absolute in situ FTIR reflectance spectra (8 cm^{-1} resolution, 100 co-added and averaged scans, 40 kHz detector speed) of the poly[Ni(saltMe)]-coated electrode in 0.1 mol dm^{-3} TEAP/CH_3CN taken at 0.1 V intervals from 0.3 to 1.3 V: a) full range spectrum, 1000 – 6600 cm^{-1} from 0.3 V i) to 1.3 V xi); b) 1000 – 1700 cm^{-1}, from 0.3 V i) to 1.3 V xi). c) Plot of the potential dependence of: (●) the absorbance of the electronic band I_E at 5600 cm^{-1}; (■) the integrated IRAV intensity ξ_I over the spectral range 1000 to 1700 cm^{-1} for both the anodic and cathodic sweeps. A = absorbance.

about 1700 cm^{-1}, resulting from the generation of charge carriers in the polymer on oxidation, and ii) selected IRAV bands in the fingerprint region, caused by the motion of the charge carriers,[16–18] which increase in intensity with increasing potential. The growth of a strong optical absorption in the near-IR region on oxidation of the polymer is entirely in accord with the concomitant decrease in the real part of the refractive index (n) mentioned above.[13] The Kramers – Kronig dispersion relations[19] clearly show that the strong absorptions at lower energies than the probing wavelength at which n is measured lead to a decrease in n.

Figure 5a – c show the absolute spectra obtained for the poly[Ni(salen)] and poly[Ni(saltMe)] films at a) 0.3 V, b) 1.0 V, and c) the difference spectra at 1.0 V, that is, the spectra

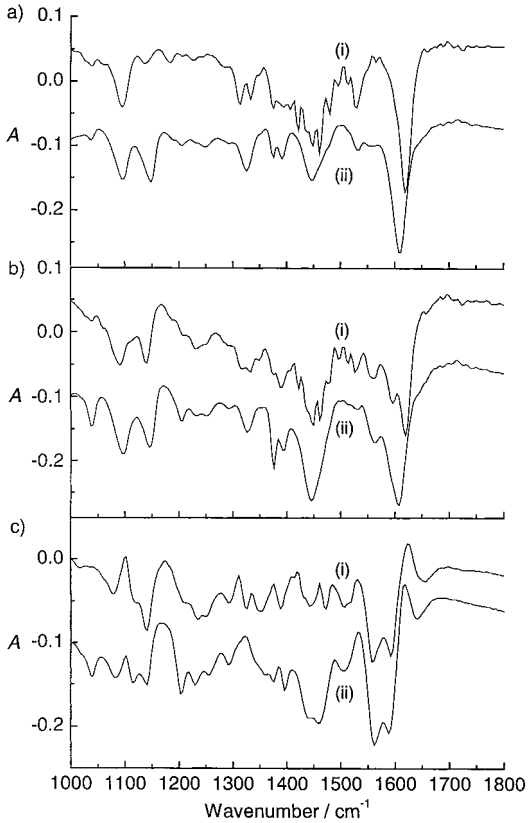

Figure 5. Absolute in situ FTIR reflectance spectra (8 cm^{-1} resolution, 100 co-added and averaged scans, 40 kHz detector speed) in the region 1000 – 1700 cm^{-1} of: i) a poly[Ni(saltMe)]-coated electrode in 0.1 mol dm^{-3} TEAP/CH_3CN; ii) poly[Ni(salen)]-coated electrode in 0.1 mol dm^{-3} TEAP/CH_3CN, taken at: a) 0.3 V, b) 1.0 V, and c) the spectra collected at 1.0 V and normalised to the spectra collected at 0.3 V. A = absorbance.

collected at 1.0 V and normalised to the relevant spectra taken at 0.3 V. In agreement with the data on the poly[Ni(salen)] films, it is clear from Figures 4a and b, and Figures 5a – c that the oxidation of poly[Ni(saltMe)] includes significant ligand involvement, with ligand features being enhanced on oxidation right across the fingerprint region (IRAV bands),[16–18] including the regions where the characteristic phenyl vibrations are expected to absorb. This provides the first indication that, although the doping level for poly[Ni(saltMe)] is 1,[11] the polymer behaves as a delocalised system (ligand-based oxidation process), rather than as a collection of discrete nickel redox centres.

By using the analysis developed for polymeric heterocycles, typified by polythiophenes,[18] and already employed in the analysis of the in situ IR data on poly[Ni(salen)],[9] the integrated intensities of all the features between 1000 and 1700 cm^{-1} (ξ_I) and the absorbance of the electronic band at 5600 cm^{-1} (I_E) were plotted as a function of potential for the anodic and cathodic stepping experiment (Figure 4c). The two plots clearly track each other, show considerable hysteresis and provide evidence for charge trapping. When the film is

0947-6539/01/0701-0142 $ 17.50+.50/0 *Chem. Eur. J.* **2001**, *7*, No. 1

held at 0.3 V for several minutes, the charge measurements and FTIR data are reproduced (Figures 1c and 4c). This implies that the difference in charge passed/IR intensity between the anodic and cathodic sweeps in a cyclic voltammogram or FTIR experiment are removed, and hence the process that gives rise to this difference is reversible with time, as would be expected for charge trapping. In addition, the behaviour at potentials > 1.1 V (see Figure 4c) is reproducible, showing that the decline in the intensities of the IRAVs and electronic band at 1.3 V was a reversible process, and not due to an irreversible "over-oxidation" of the film.[16] The maxima in the anodic and cathodic sweeps in Figure 4c occur at approximately the same potentials as the anodic and cathodic peaks in the cyclic voltammogram in Figure 1b, and have roughly the same intensities. These observations suggest that the amount of species that are produced initially during the anodic sweep, increase when cathodic charge is being passed during the cathodic sweep.

Figure 6a and b show the spectra in Figure 4a and b collected at potentials above 0.8 V (i.e. in the region of the inflexion on the anodic sweep of the cyclic voltammogram),

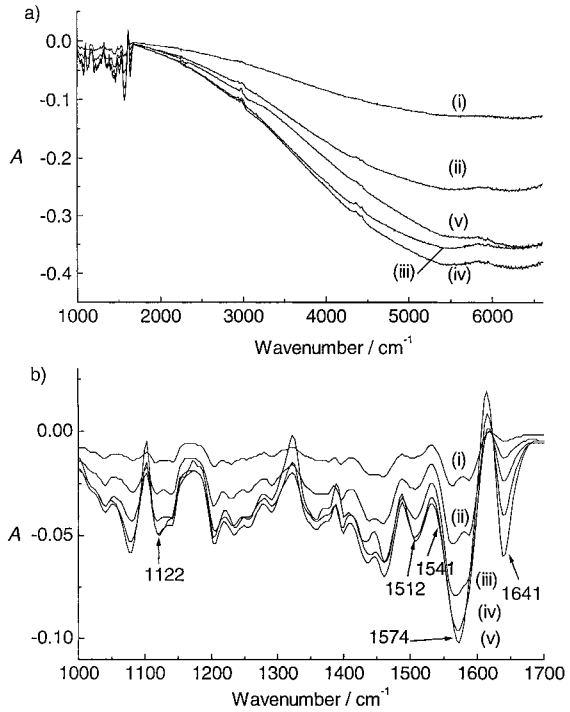

Figure 6. The in situ FTIR reflectance spectra in Figure 4 collected at potentials above 0.8 V normalised to the spectrum taken at 0.8 V: a) 1000–6600 cm^{-1} from 0.9 V (i) to 1.3 V (v); b) 1000–1700 cm^{-1}, from 0.9 V (i) to 1.3 V (v). A = absorbance.

but normalised to that taken at 0.8 V. It is clear that the features seen to increase in intensity as the film is oxidised up to 1.2 V, assigned to species A, are lost at the higher potentials, whilst there is a gain of new features near 1122, 1512, 1541, 1574 and 1641 cm^{-1}, although these are significantly weaker in intensity, as may be seen from Figure 6b. These new features, which we assign to species B, are more clearly seen in the spectrum collected at 1.3 V normalised to that taken at 1.1 V (Figure 7a and b). In this spectrum the absorptions of species

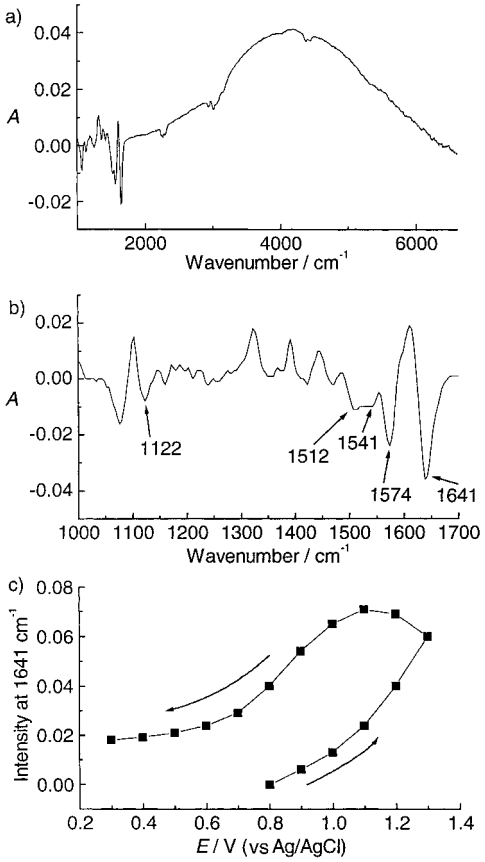

Figure 7. The in situ FTIR reflectance spectrum taken at 1.3 V in Figure 4 and normalised to that collected at 1.1 V: a) 1000–6600 cm^{-1} and b) 1000–1700 cm^{-1}. c) Plot of the intensity of the 1641 cm^{-1} feature in Figure 4 versus potential for both the anodic and cathodic sweeps. A = absorbance.

A appear as *loss* features, and the absorptions of the new species, B, are easily seen as gains. On reversing the direction of the potential steps, these new features increase in intensity until 1.1 V, after which they decrease; again, they do not return to baseline. Figure 7c shows a plot of the intensity of one of the representative bands of the species B, that at 1641 cm^{-1} as a function of potential for both the anodic and cathodic stepping experiments.

Analysis of Figure 7a suggests that the loss of A at higher potentials has an electronic feature associated with it, with a maximum near 4000 cm^{-1}. However, from Figure 7a we can deduce that the amount of A converted to B is very small. The electronic band intensity at potentials higher than 0.8 V is high, and so subtracting the spectrum at 0.8 V from that at 1.3 V means that the actual shape of the electronic loss feature cannot be judged accurately. That the intensity at 4000 cm^{-1} in Figure 4a, the frequency of the apparent maximum in Figure 7a, tracks exactly that of the maximum near 5600 cm^{-1}, suggests that the electronic loss band in the spectrum collected at 1.3 V in Figure 7a is indeed distorted. The above discussion suggests a charging mechanism of the form depicted in Scheme 1, where N is the neutral polymer, A and B are the charge carrier species defined above, and the small letters are stoichiometric coefficients.

The behaviour of the band near about 1100 cm^{-1} in Figure 4b is interesting as it appears to increase in intensity

$cN \rightarrow dA$ (0.3 – 1.2 V)

$eA \rightarrow fB + (d-e)A$ (1.2 – 1.3 V)

$gN \rightarrow hB$ (0.8 – 1.3 – 1.1 V)

$fB \rightarrow jA$ (1.3 – 0.8 V)

$(h-f)B \rightarrow kN$ (1.1 – 0.8 V)

$(d-e+j)A \rightarrow lN$ (0.8 – 0.3 V)

$(f+h) \ll (k+l) < c$

Scheme 1.

and broaden as the potential is increased; this is due to the fact that there are actually three features in this region, near 1100 cm^{-1}, 1085 cm^{-1} and 1115 cm^{-1}. The feature near 1100 cm^{-1} is potential independent, whilst the intensities of the other two features increase as the film is oxidised. The behaviour of the 1085 cm^{-1} and 1115 cm^{-1} bands may be more clearly observed in difference spectra, that is where the spectra collected during the experiment depicted in Figure 4b at potentials > 0.3 V are normalised to that taken at 0.3 V, (see Supporting Information; Figures S1 a) and b)). The sharp upward rise in the spectra between the 1085 cm^{-1} and 1115 cm^{-1} features is due to the underlying, and unmoving, 1100 cm^{-1} band; this effectively renders an accurate frequency determination of the features either side difficult. In situ FTIR spectra of poly[Ni(saltMe)] films in acetonitrile using tetraethylammonium hexafluorophosphate as the supporting electrolyte show almost identical features to those in Figure 4b (and S1 b in the Supporting Information), except that the bands near 1100 cm^{-1}, 1085 cm^{-1} and 1115 cm^{-1} are absent. Given that ClO_4^- is known to absorb near 1100 cm^{-1}, and the feature splits on co-ordination,[20] we attribute the 1100 cm^{-1} band to ClO_4^- in solution in the thin layer, and the other two features to ClO_4^- drawn into the polymer film on oxidation. Figure 8 shows a plot of the area

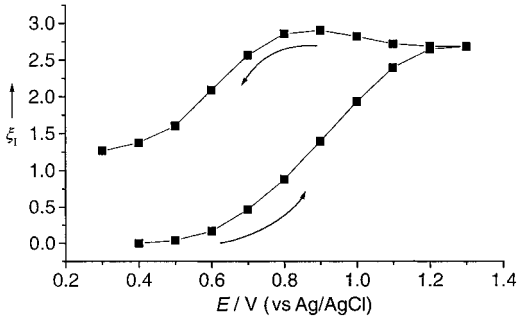

Figure 8. Plot of the potential dependence of the integrated IRAV intensity ξ_I at 1085 cm^{-1} for both the anodic and cathodic sweeps, obtained from the in situ FTIR reflectance spectra of the poly[Ni(saltMe)]-coated Pt electrode in 0.1 mol dm^{-3} TEAP/CH_3CN normalised to that collected at 0.3 V (Figure S1; see Supporting Information).

under the 1085 cm^{-1} band as a function of potential during the oxidation and subsequent reduction of the poly[NisaltMe] film, calculated from the difference spectra (as in Figure S1 a in the Supporting Information). The plot clearly shows the charge trapping and potential dependent behaviour expected on the basis of the data discussed above, and in agreement with the EQCM/PBD paper.[12]

From Figure 5a – c, it can be seen that the −C=N stretch near 1610 cm^{-1}[9, 14] occurs 10 cm^{-1} lower in the poly-[Ni(saltMe)] spectra than in poly[Ni(salen)], as would be expected when the R groups of $-C{=}N-CR_2-$ are changed from H to CH_3. In contrast, the two next highest features in frequency, near 1550 and 1601 cm^{-1}, occur at the same values in both poly[Ni(salen)] and poly[Ni(saltMe)] films. These bands have been attributed to the inter-ring phenyl C−C stretch and to the quinonoid C=C stretch,[21] respectively, and are not expected to be effected by changing the nature of the bridge between the −C=N− groups.

From Figure 4b and S1 b (see Supporting Information), it can be seen that the bands near 1328 and 1534 cm^{-1} decrease in intensity on film oxidation: the former is reasonably intense in the polymer at 0.3 V, whilst the latter, though somewhat weaker, has almost completely disappeared at 1.1 V (Figure S1; Supporting Information). Figure 9 shows the reflectance

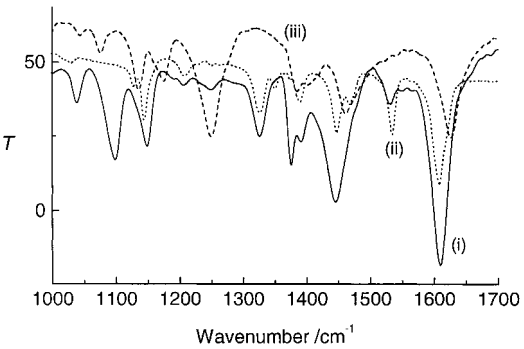

Figure 9. Comparison of: i) the absolute in situ FTIR reflectance spectrum of poly[Ni(saltMe)] taken at 0.3 V, and the FTIR transmission spectrum in KBr pellets of; ii) the monomer, [Ni(saltMe)], and iii) the ligand H_2saltMe. T = transmittance.

spectrum of the polymer at 0.3 V, and the transmittance spectra of the monomer and free H_2saltMe ligand in KBr pellets. From Figure 9 it can be seen that the bands at 1328 and 1534 cm^{-1} are absent in the free ligand spectrum, suggesting that they are due to a vibration introduced by the metal ion. A similar effect was noted in the IR spectra of a complex related to [Ni(salen)], in which the CH_2–CH_2 bridge was replaced by a benzene ring:[14] a band near 1345 cm^{-1} in the spectrum of the complex was absent from the spectrum of the free ligand, and was attributed to a vibration of the six-membered chelate ring formed by the metal ion and the co-ordinated ligand atoms.

The dependence of the intensities of the two loss features near 1328 and 1534 cm^{-1} on the potential suggests that they are not due to the same vibration or group (see Figure S2 in the Supporting Information): the band at 1328 cm^{-1} appears to follow the behaviour of the IRAVs/electronic band, whereas that at 1534 cm^{-1} is somewhat bizarre and difficult to explain.

In our previous work on poly[Ni(salen)],[9] it was found that there were three carriers formed during the oxidation up to 1.1 V. However, this was not found to be the case with the poly[Ni(saltMe)] film. All the IRAV bands have shown essentially the same behaviour as that seen in Figure 4c, with

0947-6539/01/0701-0144 $ 17.50+.50/0 *Chem. Eur. J.* **2001**, *7*, No. 1

the intensity of any feature only decreasing in the cathodic sweep at potentials < 0.8 V, despite appreciable cathodic current flowing at potentials < 1.0 V. Moreover, plots of $1/\xi_I$ versus $1/\xi_E$ were linear over the potential range 0.6–1.1 V, and with zero intercept, (see, for example, Figure S3 in the Supporting Information which shows the plot for the 1122 cm^{-1} feature). This suggests a single dominant charge carrier up to 1.1 V, (in agreement with the EPR data, see below), and that neither carrier–carrier interaction nor mean chain length dominates the observed behaviour.[18, 22, 23] The very small amount of species *B*, generated at potentials > 0.8 V, is insufficient to influence the $1/\xi_I$ versus $1/\xi_E$ plots, and it is by no means proven that B is a carrier.

In situ UV/Vis spectroscopy: The transmission spectra acquired during the deposition of a [Ni(saltMe)] film by cycling the working electrode between 0.0–1.3 V, reveal a new band at $\lambda = 475$ nm for potentials higher than 0.9 V in the positive going scan, corresponding to the beginning of the oxidation (see Figure S4, Supporting Information). The intensity of this band increases until it reaches a maximum at 1.0 V on the negative scan (beginning of the cathodic wave) and then starts to decrease. At the end of the cycle, there is an increase in absorbance over the full spectral range due to the film formation.

After the electrodeposition, the modified electrodes were transferred to monomer-free CH_3CN solutions, cycled from 0.0–1.3 V at 0.01 Vs^{-1}, and electronic spectra collected at 0.1 V intervals. Figure 10a shows the spectra of the film in the neutral state (obtained at 0.0 V) as well as that of the monomer. Both spectra are qualitatively similar and typical of Ni^{II} compounds in a square-planar geometry. They show a broad low intensity band at $\lambda \approx 550$ nm (assigned to the three unresolved d-d electronic transitions, $d_{xy} \leftarrow \{d_{z^2}; (d_{yz}, d_{xz})$, and $d_{x^2-y^2}\}$),[24] and medium and high intensity bands at $\lambda < 450$ nm (due to CT and intraligand transitions) that are shifted to slightly lower wavelengths in the polymer. The similarity between the monomer and polymer spectra provides an indication that the co-ordination sphere of nickel remains unchanged upon polymerisation.

As the polymer is oxidised, the accumulated spectra show an isosbestic point at $\lambda = 371$ nm, and an increase in intensity in the regions around $\lambda \approx 400$, 500 and > 820 nm, and a decrease in absorbance for the region $\lambda = 320$ nm (Figure 10b). By depicting the latter spectra as differential spectra, referenced to that of the polymer in the neutral state, Figure 10c, two different behaviours for the electronic band absorbances can be observed above 0.5 V in the positive going scan: 1) a decrease of the band at $\lambda = 320$ nm; 2) and an increase in absorbance for the bands at $\lambda = 404$, 440(sh), 527, and > 820 nm (high-energy edge of a band extending into the near-IR).

In order to get information on the near-IR region electronic bands, we have used a spectrometer capable of recording spectra at higher wavelengths. However, the scanning mode of this instrument required us to obtain spectra at fixed potentials, instead of dynamically during potential cycling. The successive transmission spectra (first of three scans) referenced to that of the [Ni(saltMe)] solution, acquired

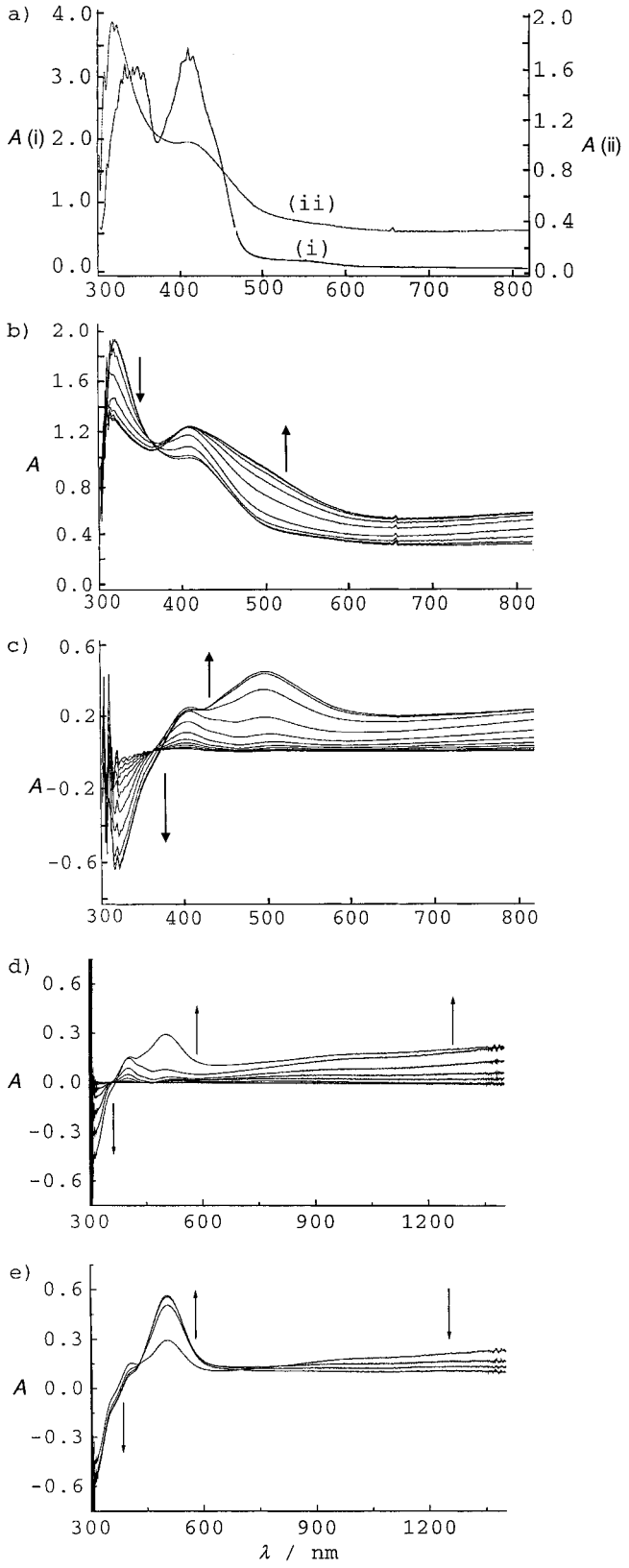

Figure 10. UV/Vis transmission spectra of a poly[Ni(saltMe)]-coated electrode in 0.1 mol dm^{-3} TEAP/CH_3CN; a) comparison between [Ni(saltMe)] (i) monomer and (ii) polymer at 0 V referenced to 0.1 mol dm^{-3} TEAP/CH_3CN; b) spectra collected from 0 to 1.3 V at 0.1 V intervals and referenced to 0.1 mol dm^{-3} TEAP/CH_3CN; c) differential spectra of b) with reference to that of the neutral polymer; differential spectra obtained during potential stepping in 0.1 V intervals from: d) 0.3 to 0.9 V, and e) 1.0 to 1.3 V. *A* = absorbance.

during a potential stepping experiment and the respective differential spectra with reference to that of the neutral polymer are shown in Figure 10d and e. These spectra are similar to those obtained by potential cycling, suggesting that the chromophores are the same and are stable, independent of the potential control function. By using a wider spectral range it was possible to see that the high-energy edge present at $\lambda >$ 820 nm in Figure 10b and c, corresponds to an electronic transition, for which the band maximum is still not defined at the edge of the spectral range used, $\lambda_{max} > 1400$ nm. Due to the similarity of the spectral range of this instrument to that of the FTIR spectrometer, it is possible to attribute unequivocally this electronic band to that observed by FTIR at ≈ 5600 cm^{-1}.

Figure 11 a – e display plots of the band absorbance from Figure 10d and e as a function of potential. We can distinguish three different patterns for band absorbance variation:

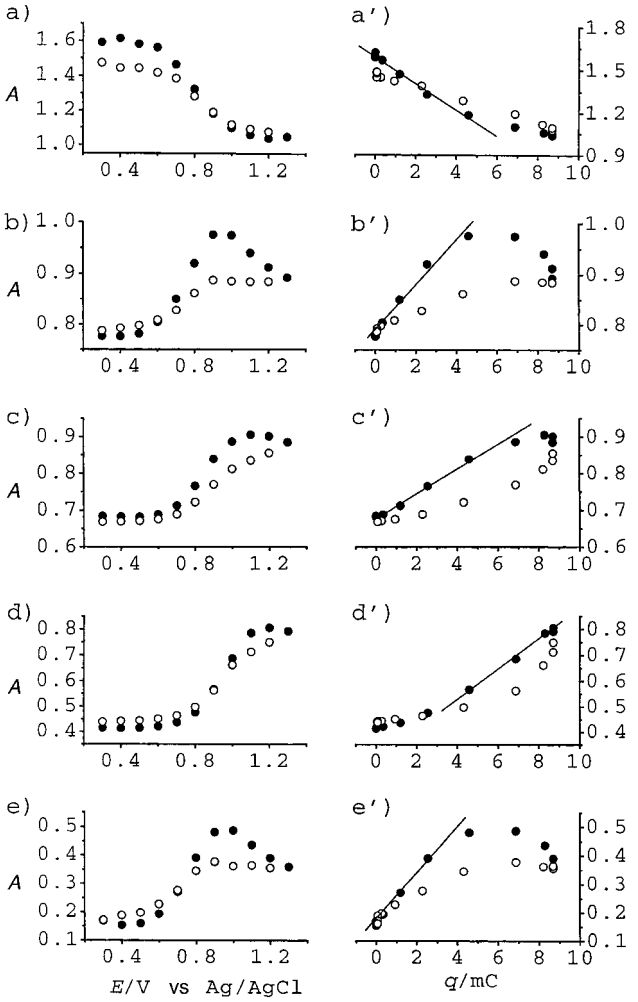

Figure 11. Plots of the absorbance of electronic bands versus E for λ_{max}: (a) 320, (b) 404, (c) 444, (d) 496 and (e) 1400 nm and plots of the diferential absorbance of electronic bands versus q for for λ_{max}: (a′) 320, (b′) 404, (c′) 444, (d′) 496 and (e′) 1400 nm. Symbols: (○) positive scan; (●) negative scan. A = absorbance.

1) bands at $\lambda_{max} = 404$ and $\lambda > 1400$ nm, start to increase at 0.5 V, reach a maximum around 1.0 V in the forward scan, and decrease thereafter until the positive potential limit (1.3 V); 2) the band at $\lambda_{max} = 527$ nm increases from 0.7 V until 1.3 V (positive potential limit), but with a continuous shift in λ_{max} (496 nm at 1.3 V); 3) the band at $\lambda_{max} = 320$ nm decreases from 0.5 V and reaches a minimum near 1.3 V. The band at 444 nm has a behaviour intermediate between the first two types: it increases from 0.5 V – 1.3 V, but decreases above 1.3 V. This suggests that its absorbance (A) versus potential (E) profile must be similar to that of the band at 404 nm, since its absorbance for $E > 0.9$ V is strongly influenced by the high intensity band at 496 nm.

Spectra obtained after several scans are identical to that of the first scan, with regard to electronic features and Abs *vs* E profiles. The corresponding cyclic voltammograms do not show any decrease in current intensity and remain reversible at the end of the potential cycling. This is an indication that the high electrochemical stability and conductivity observed for the polymer in CH_3CN/0.1 mol dm^{-3} TEAP and in the potential range 0 – 1.3 V, have parallels in the high stability of film electronic structure. Moreover, as the first cycle effect detected in the electrochemical studies[11] and in the combined EQCM/PBD data[12] has no correspondence in the UV/Vis spectra, it may be concluded that it must be associated with structural/morphological polymer rearrangements, and not changes in the electronic structure of the polymer. Spectra acquired during potential cycling or stepping, for films of different thickness, show the same electronic features, the same A versus E profiles, and the same stability patterns.

Electronic spectra were also acquired during film redox switching in DMF and $(CH_3)_2SO$ to study the behaviour in these strongly co-ordinating solvents. In the first scan the respective differential spectra show the same electronic bands and the same A versus E profiles as those observed in CH_3CN, but with a significant decrease in absorbance; the corresponding cyclic voltammograms show one irreversible process at 0.93 V. In subsequent scans a substantial decrease in current intensity and absorbance is observed; furthermore, when no electrochemical responses are detected, no electronic bands are observed during the positive potential half cycle. As the polymer remains at the electrode surface, these observations suggest that the polymer became electroinactive and hence, all the bands observed in the electronic spectra during redox switching are related to polymer electroactivity. In these strongly co-ordinating solvents, interactions between the solvent molecules and the nickel centre may occur, which induce a significant change in the polymer electronic structure and breaking of the ligand π-delocalised system. No evidence for oxidation of the metal centre could be found in the EPR spectra (see below) for polymers conditioned in these solvents, confirming the electroinactivity of the resulting nickel polymer.

Another point is that the electronic band maxima and A versus E profiles observed in CH_3CN exactly match those observed for poly[Ni(salen)][9] (for the same potential range) and for other similar nickel polymers with different imine bridges.[25] The same electronic bands, although with band maxima shifted to slightly higher energies and similar A versus E profiles, are also observed for the homologous copper-based polymers.[26]

By coupling of coulometric data (extracted from the voltammograms) with the absorbance of the different bands

0947-6539/01/0701-0146 $ 17.50+.50/0 *Chem. Eur. J.* **2001**, *7*, No. 1

for the redox switching in CH_3CN (Figure 11a′–e′), it is possible to estimate the molar extinction coefficients ε (λ)/ $mol^{-1}\,dm^3\,cm^{-1}$ for each electronic band by using Equation (1), where F is the Faraday constant and q ($C\,cm^{-2}$) is the

$$A(\lambda)=\frac{\varepsilon(\lambda)q}{nF} \quad (1)$$

charge density. Estimates of the molar extinction coefficients for the electronic bands at 320, 404, 444, 496 and 1400 nm were obtained from the slopes of straight-line regions where absorbance changes are maximal in Figure 11a′–e′. Using the value of $n=1$ for the number of electrons transferred per monomer unit obtained by the coulometric data,[11] the following values were calculated: $\varepsilon(320\,nm)\approx 7100\,mol^{-1}\,dm^3\,cm^{-1}$, $\varepsilon(404\,nm)\approx 3100\,mol^{-1}\,dm^3\,cm^{-1}$, $\varepsilon(444\,nm)\approx 2700\,mol^{-1}\,dm^3\,cm^{-1}$, $\varepsilon(496\,nm)\approx 7100\,mol^{-1}\,dm^3\,cm^{-1}$ and $\varepsilon(1400\,nm)\approx 5200\,mol^{-1}\,dm^3\,cm^{-1}$. These values are similar to those obtained for poly[Ni(salen)][9] and provide a strong indication that these electronic bands, which are associated with charge conduction within the polymer, must correspond to electronic transitions betweeen states that have large contributions from ligand-based orbitals. This confirms that polymer oxidation is a ligand based process.

EPR spectroscopy: Poly[Ni(saltMe)] films exhibit EPR spectra with only one radical-type isotropic signal at $g=$ 2.007 with a peak-to-peak distance of 0.25 mT (Figure 12a).

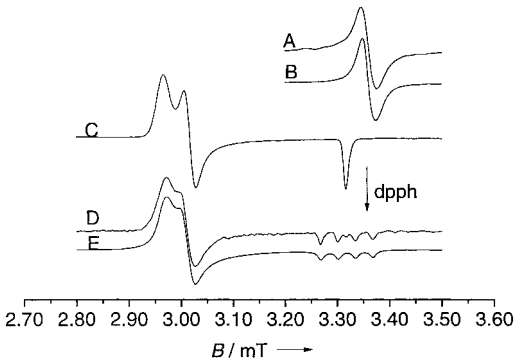

Figure 12. Ex situ EPR spectra at 77 K of: a) poly[Ni(saltMe)] in the oxidized state obtained; b) poly[^{61}Ni(saltMe)] obtained under the same conditions as a); c) [Ni(saltMe)] oxidized in $(CH_3)_2SO$ by constant-potential electrolysis at 1.3 V; d) [^{61}Ni(saltMe)] obtained under the same conditions as c); e) Simulation of the spectrum d.

The signal intensity depends on the potential (low intensity for the neutral state and high intensity for oxidised state) and on the temperature (the spectra are much more intense at 77 K).

The isotropic radical-type EPR spectra can be compared with those obtained for the oxidised monomeric species in DMF and $(CH_3)_2SO$ (Figure 12c), which are typical of metal centred oxidised species, with large g tensor anisotropy and g_{av} in the range of 2.167–2.170 [$g_{av}=1/3(g_x+g_y+g_z)$],[10] and that have been attributed to the Ni^{III} six-co-ordinate complexes $[Ni^{III}(saltMe)(DMF)_2]^+$ and $[Ni^{III}(saltMe)((CH_3)_2SO)_2]^+$. The comparison between the spectra obtained for the oxidised species in the strongly co-ordinating solvents and in CH_3CN indicates that the polymerisation and electroactivity of poly[Ni(saltMe)] in the latter solvent are ultimately ligand-centred processes, even for this polymer which has a doping level of 1.

In order to highlight the role of the nickel centre in the electronic structure of the polymer, we have electrosynthesised the polymer from ^{61}Ni-enriched monomer and obtained its EPR spectrum. The EPR spectrum of poly[^{61}Ni(saltMe)] (Figure 12b) obtained in the same experimental conditions as those for naturally abundant nickel polymers, does not exhibit any detectable hyperfine couplings or line broadening due to coupling of the unpaired electron with the ^{61}Ni ($I=3/2$) centre. For comparison, we have also obtained the EPR spectra of the ^{61}Ni enriched oxidised monomeric complexes in $(CH_3)_2SO$. The spectrum shows the same g values as those of the natural abundant complex ($g_x=2.263$, $g_y=2.230$ and $g_z=$ 2.026), but exhibits well resolved ^{61}Ni hyperfine splittings in the high field region (one quartet with $|A_z|^{61}Ni=33.24$ gauss), and a small broadening of the g_x and g_y signals, due to the unresolved hyperfine couplings in this region ($|A_x|=|A_y|$ $^{61}Ni=5.00$ gauss).

The EPR spectrum for the enriched polymer proves conclusively that there is no Ni^{III} in the oxidised polymer (even for the high potential used) and that no direct detectable interaction between the nickel centre and the unpaired spin takes place. However, small indirect interactions between the metal and the unpaired spin (by polarisation mechanisms) can not be excluded, as the large bandwidth that characterises the powder solid-state EPR spectra may be responsible for the non-observance of any change in the ^{61}Ni-enriched polymer spectra when compared with those of natural abundance nickel polymer spectra. The delocalised π-ligand system responsible for the conduction may probably include the nickel centre, but with the nickel acting only as an innocent bridging atom between the two phenyl rings of the monomer. That the conduction path may be very close to or include the nickel atom is also suggested by the FTIR, as the intensity of vibrations due to the six-membered chelate ring is strongly affected during redox switching.

The EPR signal of polymers in the neutral state (obtained either by potential cycling ending at 0.0 V, or by electrolysis at 1.3 V followed by equilibration at 0.0 V) is six times less intense than that of polymers in the oxidised state (at 1.0 or 1.3 V). This is another indication of the occurrence of spin trapping, observed using FTIR. Moreover, no other EPR signal was detected in experiments where the polymer was obtained at 1.3 V and then conditioned for 5 min at three different potentials (1.0, 1.3 and 1.6 V). These results point to formation of a single type of ligand-based paramagnetic species during polymer oxidation, as has been suggested by FTIR data, and can be compared with the EPR spectra of poly[Ni(salen)], for which three signals have been detected.[9]

EPR spectra of polymers conditioned in $(CH_3)_2SO$ at positive potentials show the same radical-type signal, but much less intense than that observed in CH_3CN. Radical signal intensity depends on conditioning time, with longer times implying less intense signals. This suggests that decomposition of radical paramagnetic species occurs in this solvent.

After several positive cycles in $(CH_3)_2SO$, the polymers have no electrochemical responses and are EPR silent.

EPR data provide direct evidence that polymerisation of [Ni(saltMe)] and film oxidation in CH_3CN are ligand-based processes, and that the paramagnetic species produced in the potential range between 0.5 and 1.3 V are responsible for the electroactivity and charge conduction in the polymers.

Conclusion

We were able to show by three independent spectroscopic techniques (in situ FTIR and UV/Vis and ex situ EPR) that polymerisation of [Ni(saltMe)] and redox switching of poly-[Ni(saltMe)] involve oxidative ligand based processes. This latter result is even more remarkable when coulometric studies have shown that one positive charge was delocalised through one monomer unity.

This non-direct interference of the metal in the oxidation process is clearly seen in the EPR data, in which identical radical-type spectra for ^{61}Ni-enriched and natural abundance Ni polymers have been observed. Although we were not able to prove unequivocally that the charge conduction is through the de-localised π system that contains the metal atom, the other possibility for charge conduction, through phenyl moieties in stacked polymers, has been excluded by ellipsometric studies.[13] The significant increase in the thickness that occurs during polymer oxidation (approximately 20 %), due to the ingress of anions and solvent into the film, will prevent any electrical conduction during redox switching.

The spectroelectrochemical studies of the homologous copper-based polymers, to be published elsewhere,[26] have shown that these polymers also have the same electronic bands, but slightly shifted to higher energies, and similar *A* versus *E* profiles. The comparison with the nickel-based polymers also suggests that the metal atom does not directly interfere in the electroactivity of the polymers, but does have a contribution to the π-delocalised system responsible for the charge conduction

Poly[Ni(salen)] and poly[Ni(saltMe)] have the same electronic bands and *A* versus *E* profiles, and furthermore the same λ_{max} for electronic bands and *A* versus *E* profiles are also observed for polymers based in nickel monomers derived from salicylaldehyde, but with other imine bridges: 2,2′-dimethylethylene – poly[Ni(saldMe)],[25] and cyclohexane – poly[Ni(salhd)].[25] These are strong indicators that the ligand active sites are associated with molecular orbitals that do not involve atoms of the imine bridge.

The coupling of the data from all the spectroscopic techniques suggests that the dominant charge carriers in poly[Ni(saltMe)] are polarons, as observed for poly[Ni-(salen).[9] In this context, we propose the polaronic model[27] to interpret the UV/Vis spectroscopic data during the doping process: the electronic band at 320 nm (3.88 eV) is assigned to the intervalence band as it decreases upon oxidation. Bands at 404, 444 nm (3.07, 2.79 eV) and at 5600 cm^{-1} (0.69 eV) show the same *A* versus *E* profile, indicative that they are associated with the same charge carriers, polarons. These three electronic bands can thus be assigned to transitions within states in the band gap generated during polymer oxidation: 1) from the valence band to the bonding polaron level (0.69 eV); 2) from the valence band to the anti-bonding polaron level (3.07 eV); 3) and from the bonding to the anti-bonding polaron level (2.79 eV).

A check for this assignment can be provided by noting that: 1) the sum of the lowest energy transitions, $2.79+0.69=3.48$ eV, is close (within 13 %) to that of the high energy band at 3.07 eV, and 2) the sum of the energy for the electronic transitions originated on the intervalence band, $3.07+0.69=3.79$ eV is close to the energy of the observed band gap (3.88 eV).

The behaviour of the band at $\lambda_{max}=527$ nm is unique and different from the bands assigned to polarons: its λ_{max} shifts with potential ($\lambda_{max}=527$ nm at 0.7 V to 496 nm at 1.3V) and the maximum in the *A* versus *E* plot is at higher potential relative to the other bands. These observations suggest that the electronic states between which we observe the electronic transitions are formed (and changing) as the polymer is oxidised, up to a potential of 1.3 V. Coupling these observations with the fact that, during polymer oxidation, a new highly delocalised π system is formed through the quinoid bond between two phenyl rings, we assign this band to a charge transfer transition between the metal and the new electronic structure of the ligand in the oxidised state.

One important feature that emerges from the comparison between poly[Ni(saltMe)] and poly[Ni(salen)] is that the similarity in their electronic structure in the reduced and oxidised state has no counterpart in their electrochemical performances and conductivity. The former polymer exhibits very high electrochemical stability and conductivity in CH_3CN/0.1 mol dm^{-3} TEAP. Replacing the hydrogen atoms in the imine bridge with methyl groups increases simultaneously the bulkiness and electron-donating properties of the substituents. However, as the conduction path does not include the imine bridge, polymer electroactivity is not strongly dependent on the electronic properties of its substituents. We can thus consider that the bulkiness of the methyl substitutents is indirectly responsible for the differences in electrochemical stability/conductivity between poly-[Ni(saltMe)] and poly[Ni(salen)]. We propose further that the steric effect is ultimately responsible for structural differences between the two films, probably arising from different film compaction.

EQCM-PBD and ellipsometry data[12, 13] have shown that poly[Ni(saltMe)] behaves as a homogenous film and that a significant increase in thickness occurs during the redox switching as a consequence of anion ingress and solvent swelling. However, similar information could not be gathered for poly[Ni(salen)], as its low electrochemical stability has prevented ellipsometry studies and the characterisation of its redox dynamics, thereby precluding direct structural comparison between the two polymers.

Some indirect insights into polymer compaction can be gained by extrapolation of the known crystal packing of their monomers. Whereas [Ni(salen)] exists as dimers with Ni···Ni intermolecular distance less than 3.5 Å,[28] in the asymmetric unit of [Ni(saltMe)] there are three independent molecules with intermolecular Ni···Ni distances longer than 5.56 Å.[29]

0947-6539/01/0701-0148 $ 17.50+.50/0 *Chem. Eur. J.* **2001**, *7*, No. 1

The differences in crystal packing have been attributed to the imine bridge methyl groups, which prevent close contact between monomers and generate an open crystal structure when compared to that of [Ni(salen)]. These repulsive forces must also be present in poly[Ni(saltMe)] and would impose an open and flexible structure, which would be responsible for the observed facile anion ingress and solvent swelling. The analogy with monomer structure would predict a more compact structure for poly[Ni(salen)] which would hinder the necessary movement of species from solution into the film associated with polymer charge transfer.

Our results suggest that the supramolecular structure of these nickel-based polymers may play a key role in the control of their electrochemical stability by governing the movement of mobile species between film and solution during redox switching. We are pursuing the characterisation (by EQCM-PBD and ellipsometry) of similar nickel polymers, in which the imine bridges have stereochemical requirements intermediate between those of salen and of saltMe, in an attempt to correlate electrochemical stability/performance with film structure.

Experimental Section

Materials: [Ni(saltMe)], 2,3-dimethyl-*N*,*N*′-bis(salicylidene)butane-2,3-diaminatonickel(II), was prepared by published procedures,[10] and recrystallised from acetonitrile. The complex [^{61}Ni(saltMe)] was prepared by addition of ethanolic solution of the ligand to an ethanolic solution of $^{61}NiNO_3$ obtained from the digestion of metallic ^{61}Ni (Oak Ridge National Laboratories) with concentrated HNO_3 (Merck p. a.).[30] Tetraethylammonium perchlorate (TEAP; Fluka, puriss) was used as received and kept in an oven at 60 °C. Acetonitrile (Fisions, HPLC grade) was refluxed twice over CaH_2 and distilled under nitrogen before use. DMF and $(CH_3)_2SO$ (Merck, pro analysi.) were used as received.

IR spectroscopy: The FTIR spectrometer employed was a BioRad FTS-60. Spectra were obtained at 8 cm^{-1} resolution, and comprised 100 co-added and averaged scans at a detector speed of 40 kHz. The FTIR spectrometer was controlled by an Oxsys Micros Electrochemical Interface, which also controlled the electrochemistry in the spectroelectrochemical cell. The spectroelectrochemical cell was of a standard three-electrode, thin-layer design, which is described in detail elsewhere.[18, 22, 23] The window employed was a 2.5 cm diameter, 0.3 cm thick CaF_2 plate. The counter electrode was a Pt gauze loop, and the reference electrode was a commercial (S.H. Scientific) Ag/AgCl electrode, separated from the cell itself by a salt bridge containing TEAP (0.1 mol dm^{-3})/CH_3CN, to minimise contamination by water. The working electrode was a solid "top hat"-shaped piece of Pt polished on the exposed face, of area 0.64 cm^2. In the difference spectra presented, a reference spectrum S_r was collected at a reference potential E_r. The potential was then stepped down or up in 0.1 V increments, and spectra S_n taken at each potential E_n, after the potential had been held for ten seconds at the specified value. The spectra are represented as $\log_{10}(S_n/S_r)$ "absorbance" versus $\tilde{\nu}$ (cm^{-1}). "Absolute" spectra, for instance of the polymer, were obtained by collecting a reference spectrum from the uncoated Pt electrode immersed in CH_3CN/0.1 mol dm^{-3} TEAP. The solution in the cell was then replaced with electrolyte containing the monomer, the polymer grown, and the growth solution replaced with CH_3CN/0.1 mol dm^{-3} TEAP. The thickness of the layer was then adjusted and the solvent absorptions monitored by using the real time display option on the spectrometer; the spectrum of the polymer was collected once the solvent absorptions had been as close as possible annulled.

UV/Vis transmission spectroscopy: We used either a Hewlett Packard HP8451 or a Perkin Elmer Lambda 19 UV/VIS/NIR spectrometer. Spectroscopic measurements were made in situ in transmission mode, with the electrode under potential control, using an Autolab PGSTAT20 potentiostat/galvanostat. The working electrode was an indium tin oxide (ITO)-coated conducting glass (Balzers) and its area (typically 2.0 cm^2) was defined by a silicone sealant (Dow Corning 3145 RTV). All potentials were measured and quoted with respect to a $Hg/HgCl_2$ (NaCl 0.1 mol dm^{-3}) reference electrode; the counter electrode was Pt gauze. The Hewlett Packard HP8451A spectrophotometer was programmed to acquire spectra at 10 s intervals in the range 300–820 nm during potential sweeping, while the Perkin Elmer spectrometer was programmed to acquire spectra in the range 300–1600 nm at fixed potentials, incremently stepped in 0.1 V intervals from 0 to 1.3 V and back to 0 V. A background spectrum (0.1 mol dm^{-3} TEAP/Solv, Solv = CH_3CN, DMF and $(CH_3)_2SO$) and a reference spectrum (1 mmol dm^{-3} [Ni(saltMe)] in 0.1 mol dm^{-3} TEAP/Solv) were collected before electrode modification.

Electron paramagnetic resonance: EPR spectra were obtained with an X-band Bruker ESP 300E spectrometer at room temperature and 77 K. Spectra were calibrated with diphenylpicrylhydrazyl (dpph; $g = 2.0037$) and the magnetic field was calibrated by use of Mn^{II} in MgO. The samples were prepared as poly[Ni(saltMe)] and poly[^{61}Ni(saltMe)]-modified Pt wires, ($\phi = 0.025$ cm) that were inserted into quartz EPR tubes ($\phi = 0.4$ cm). The EPR parameters were obtained by simulation using the programme Win EPR Simfonia (Bruker).

Methods: Poly[Ni(saltMe)] films for UV/Vis and for FTIR measurements were deposited by cycling the potential of the working electrode between 0.0 and 1.3 V of a CH_3CN solution 1 mmol dm^{-3} in [Ni(saltMe)] monomer and 0.1 mol dm^{-3} TEAP; scan rates were 0.01 or 0.1 V s^{-1} for UV/Vis and 0.1 V s^{-1} for FTIR studies. After electropolymerisation, the modified electrode was rinsed thoroughly with dry CH_3CN and the experiments were carried out on films immersed in solutions 0.1 mol dm^{-3} TEAP; the solvents were CH_3CN, DMF, and $(CH_3)_2SO$ for UV/Vis and CH_3CN for FTIR. Films with different thickness were prepared by changing the number of potential cycles used. The electroactive polymer surface coverage for each film, Γ (mol cm^{-2}), was obtained by coulometric assay in monomer-free solution under the assumption that one positive charge is delocalised per one monomer unit.[11] The voltammograms used in the calculation of the electroactive surface coverage were performed at 0.01 V s^{-1}.

Poly[Ni(saltMe)] and poly[^{61}Ni(saltMe)] films for EPR studies were produced by different methodologies depending on the desired redox state: 1) films were obtained by cycling the potential between 0.0 and 1.3 V and ending at 0.0 V (neutral state); 2) films were produced by holding the potential of the working electrode at 1.0 V or 1.3 V for 15 or 10 min, respectively (oxidised states); 3) films were obtained by holding the potential at 1.3 V for 10 min in a solution containing the monomer, and then transferred to a monomer-free CH_3CN solution and the potential was held for 5 min at 0 V (neutral state), 1.0 V, 1.3 V, and 1.6 V (oxidised states), and 4) films were obtained at 1.3 V and then transferred to a $(CH_3)_2SO$ monomer free solution and the potential held at 1.3 V for 5 min. After preparation the films were immediately inserted in EPR tubes.

Acknowledgements

This work was partially supported by the "Fundação para a Ciência e Tecnologia" through Project PBIC/QUI/2137/95. M.V.B. thanks the FCT/Praxis XXI for a fellowship.

[1] K. A. Goldsby, *J. Coord. Chem*. **1988**, *19*, 83–90.
[2] K. A. Goldsby, L. A. Hoferkamp, *Chem. Mater*. **1989**, *1*, 348–352.
[3] P. Audebert, P. Hapiot, P. Capdevielle, M. Maumy, *J. Electroanal. Chem. Interfacial Electrochem*. **1992**, *338*, 269–278.
[4] P. Audebert, P. Capdevielle, M. Maumy, *New J. Chem*. **1992**, *16*, 697–703.
[5] M. Maumy, P. Capdevielle, P. H. Aubert, P. Audebert, M. Roche, *New J. Chem*. **1997**, *21*, 621–626.
[6] F. Bedioui, E. Labbe, S. Gutierrez-Granados, J. Devynck, *J. Electroanal. Chem. Interfacial Electrochem*. **1991**, *301*, 267–274.
[7] C. E. Dahm, D. G. Peters, J. Simonet, *J. Electroanal. Chem*. **1996**, *410*, 163–171.
[8] C. E. Dahm, D. G. Peters, *J. Electroanal. Chem*. **1996**, *406*, 119–129.

  0947-6539/01/0701-0149 $ 17.50+.50/0

[9] M. Vilas-Boas, C. Freire, B. Castro, A. R. Hillman, P. A. Christensen, *Inorg. Chem*. **1997**, *36*, 4919 – 4929.
[10] C. Freire, B. Castro, *J. Chem. Soc. Dalton Trans*, **1998**, 1491 – 1497.
[11] M. Vilas-Boas, C. Freire, B. Castro, A. R. Hillman, *J. Phys. Chem. B* **1998**, *102*, 8533 – 8540.
[12] M. Vilas-Boas, M. Henderson, C. Freire, B. Castro, A. R. Hillman, E. Vieil, *Chem. Eur. J.* **2000**, *6*, 1160 – 1167.
[13] J. C. Abel, M. Vilas-Boas, C. Freire, A. Hamnett, P. A. Christensen, unpublished results.
[14] M. Dutta, D. H. Brown, W. E. Smith, *Spectrochim. Acta A* **1983**, *39*, 37 – 42.
[15] I. C. Santos, M. Vilas-Boas, C. Freire, B. Castro, P. A. Christensen, A. R. Hillman, unpublished results .
[16] T. Hattori, W. Hayes, K. Wong, K. Kaneto, K Yoshino, *J. Phys. Chem.* **1984**, *17*, L803.
[17] P. A. Christensen, A. Hamnett, *Electrochim. Acta* **1991**, *36*, 1263 – 1286.
[18] P. A. Christensen, A. Hamnett, A. R. Hillman, M. J. Swann, S. J. Higgins, *J. Chem. Soc. Faraday Trans.* **1992**, *88*, 595 – 604.
[19] A. S. Davydov, *Quantum Mechanics*, Pergamon, Oxford, England, **1965**.
[20] G. Socrates, *Infrared Characteristic Group Frequencies*, Wiley, Bath, England, **1980**.
[21] M. C. Pham, S. Aeiyach, J. Moslih, P. Soubiran, P. C. Lacaze, *J. Electroanal. Chem. Interfacial Electrochem*. **1990**, *277*, 327 – 336.
[22] P. A. Christensen, A. Hamnett, A. R. Hillman, M. J. Swann, S. J. Higgins, *J. Chem. Soc. Faraday Trans.* **1993**, *89*, 921 – 926.
[23] P. A. Christensen, A. Hamnett, D. C. Read, *Synth. Met*.**1994**, *62*, 141 – 152.
[24] a) A. B. P. Lever, *Inorganic Electronic Spectroscopy*, 2nd ed, Elsevier, New York, **1984**; b) G. Maki, *J. Chem. Phys.* **1958**, *28*, 651 – 662; c) G. Maki, *J. Chem. Phys.* **1958**, *28*, 1129 – 1138.
[25] I. C. Santos, M. Vilas-Boas, C. Freire, B. Castro, A. R. Hillman, unpublished results.
[26] M. Martins, M. Vilas-Boas, C. Freire, B. Castro, A. R. Hillman, unpublished results.
[27] J. Bredas in *Handbook of Conducting Polymers* (Ed.: T. J. Skotheim), Marcel Decker, New York, **1986**, Chapter 25.
[28] A. G. Manfredotti, C. Gusatini, *Acta Crystallogr. Sect. C* **1983**, *39*, 863 – 865.
[29] I. C. Santos, M. Vilas Boas, M. F. M. Piedade, C. Freire, M. T. Duarte, B. de Castro, *Polyhedron*, **2000**, *19*, 655 – 664.
[30] D. Lexa, M. Momenteau, J. Mispelter, J. M. Savéant, *Inorg. Chem.* **1989**, *28*, 30 – 35.

Received: March 21, 2000 [F2376]